

RainNet: A Large-Scale Dataset for Spatial Precipitation Downscaling

Xuanhong Chen^{1,*}, Kairui Feng^{2,*}, Naiyuan Liu^{3,**}, Yifan Lu^{1,**}, Zhengyan Tong¹,
Bingbing Ni^{1,†}, Ziang Liu¹, Ning Lin²

¹Shanghai Jiao Tong University, ²Princeton University, ³University of Technology Sydney

{chen19910528, yifan_lu, 418004, nibingbing, acemenethil}@sjtu.edu.cn

{kairuif, nlin}@princeton.edu, naiyuan.liu@student.uts.edu.au

Abstract

*Spatial Precipitation Downscaling is one of the most important problems in the geo-science community. However, it still remains an unaddressed issue. Deep learning is a promising potential solution for downscaling. In order to facilitate the research on precipitation downscaling for deep learning, we present the first **REAL** (non-simulated) Large-Scale Spatial Precipitation Downscaling Dataset, **RainNet**, which contains **62,424** pairs of low-resolution and high-resolution precipitation maps for 17 years. Contrary to simulated data, this real dataset covers various types of real meteorological phenomena (e.g., Hurricane, Squall, etc.), and shows the physical characters - **Temporal Misalignment**, **Temporal Sparse** and **Fluid Properties** - that challenge the downscaling algorithms. In order to fully explore potential downscaling solutions, we propose an implicit physical estimation framework to learn the above characteristics. Eight metrics specifically considering the physical property of the data set are raised, while fourteen models are evaluated on the proposed dataset. Finally, we analyze the effectiveness and feasibility of these models on precipitation downscaling task. The Dataset and Code will be available at <https://neuralchen.github.io/RainNet/>.*

1. Introduction

The geoscience community's classical understanding treats the earth system as a deterministic but extensive physical system, where the law of every particle is pre-known. Following this line, global weather prediction, as a computational problem, is comparable to the simulation of the human brain and the evolution of the early Universe, and it is performed every day at major operational centers across the world [3]. The improvement of the weather forecast and Geo-data quality saves tremendous money and lives; with

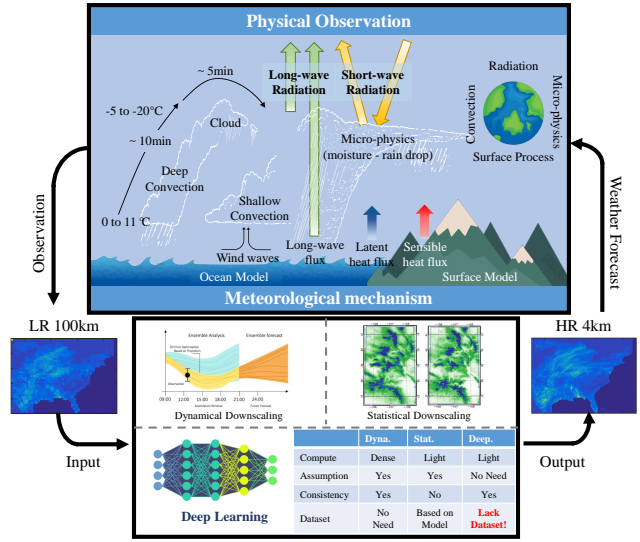


Figure 1. Downscaling is a vital task in geo-science, which involves complex physical processes. Deep learning framework is one potentially promising solution, comparing to computational dense dynamic methods and spatial-temporal non-consistent statistical methods. No formal dataset challenges the application of deep learning in downscaling. In contrast to simulated toy-dataset, our RainNet contains more than 36000 low- and corresponding high-resolution precipitation map pairs.

the fiscal year 2020 budget over \$1 billion, NSF funds thousands of colleges in U.S. to research on these topics [22]. However, in recent years, with computer science development, a deluge of Earth system data is continuously being obtained, coming from sensors all over the earth and even in space. These ever-increasing massive amounts of data, coming in different sources and structures, challenge the geoscience community, which lacks practical approaches to understand and further utilize the data and a flexible framework with less pre-knowledge constraints to blend the data [24] (Shown in Fig. 1).

At the same time, deep learning has made an enormous breakthrough in the field of computer vision, which is ex-

*Equal contribution. **Equal contribution. † Corresponding author.

tremely good at extracting valuable knowledge from numerous amounts of data. Witnessing such a situation, several preliminary works [9, 34, 12] try to introduce machine learning and deep learning tools to solve meteorological problems, *e.g.*, spatial precipitation downscaling (increasing resolution of initial coarse precipitation dataset, which plays a vital role in daily weather prediction). However, these methods are only applied to ideal retrospective problems and verified on simulated datasets (*e.g.*, bi-cubic of precipitation generated by weather forecast model on historical events [4]), which significantly weakens the credibility of the feasibility and effectiveness of the methods. To efficiently develop the massive geo-data and speed up the deep learning research for geosciences, we build the first large-scale *spatial precipitation downscaling* dataset for deep learning. Furthermore, we propose an implicit dynamic estimation model as a baseline model to explore potential downscaling solutions.

The precision of weather prediction is highly dependent on the resolution and reliability of the initial environmental input variables, which drives complex physical weather projection models. If the input dataset is nine-times higher resolution, the output will show at least nine-times details. However, the raw data for weather prediction is usually from multi-sources with different levels of confidence. Scientists generally average the raw data to coarse spatial scales (*i.e.*, 25 to 100km), which are hard to resolve many fine-scale meteorological phenomena (*e.g.*, hurricane, regional rainstorm, *etc.*). The conventional solution for this issue is *Spatial Downscaling*, whose main task is to infer higher resolution information from raw meteorological data.

There are three mainstream spatial downscaling forms: 1). *Dynamical Downscaling*, it infers the fine-scale precipitation and other climate statues via simulating the fine-scale/regional dynamic process of the coupled land-atmosphere system abstractly described by regional numerical weather or physical climate models. Dynamical downscaling usually demands massive computational resources and also needs to set a large number of empirical parameters [1], leading to poor timeliness and model performance.

2). The second form is *Statistical Downscaling* approaches, which aim to establish statistical relationships between small and large-scale meteorological variables. Since their simplicity and low computational cost overhead, the statistical downscaling forms an attractive alternative to dynamical one [12]. However, statistical downscaling results usually lack of physical logic lies behind different atmospheric phenomena in space and time. Simultaneously, the data contain high uncertainty that impacts the quality of weather forecasts driven by statistical downscaling methods [16].

3). Compared to the above two long-developed forms,

Deep-learning Downscaling is in its infancy, but has shown superior performance and reasonable computational resource overhead. Nevertheless, the existing deep learning methods [9, 34] have NO real and well-organized geo-dataset for training, resulting in the low-confidence model performance in real-world scenarios. Furthermore, these methods fail to effectively learn spatio-temporal dynamic properties, which is the most critical and fundamental in spatial downscaling.

To overcome the shortages of existing deep-learning downscaling pipelines, we build the first well-organized large-scale spatial precipitation downscaling dataset for deep learning, dubbed *RainNet*. RainNet provides rainy season precipitation data for 17 years (*i.e.*, 2002 ~ 2018) in the eastern United States, including 62,424 pairs of low-resolution and high-resolution data. These data are collected from satellites, radars and gauge stations, which can reveal the multi-source characteristics of meteorological data. In detail, the multi-source characteristics make the meteorological data show serious *Temporal Misalignment* and *Temporal Sparse* problems, which are more challenging than the image/video super-resolution problem. Unlike video super-resolution, the motion of precipitation region is non-rigid (*i.e.*, fluid), while video super-resolution mainly concerns about rigid body motion estimation. To fully explore how to alleviate the mentioned predicament, we propose an implicit dynamics estimation downscaling model. Our model hierarchically aligns adjacent precipitation maps, that is, implicit motion estimation. It is very simple but exhibits very competitive performance. The main contributions of this paper are:

- To the best of our knowledge, we present the first REAL (non-simulated) Large-Scale Spatial Precipitation Downscaling Dataset for deep learning; Simultaneously, we deeply analyze the physical characteristics and challenges of the dataset;
- We propose a downscaling model with strong competitiveness;
- We evaluate 14 competitive potential solutions on the proposed dataset, and analyze the feasibility and effectiveness of these solutions.

2. Background

At the beginning of the 19th century, geoscientists recognized that predicting the state of the atmosphere could be treated as an initial value problem of mathematical physics, wherein future weather is determined by integrating the governing partial differential equations, starting from the observed current weather. Today, this paradigm translates into solving a system of nonlinear differential equations at about half a billion points per time step and accounting

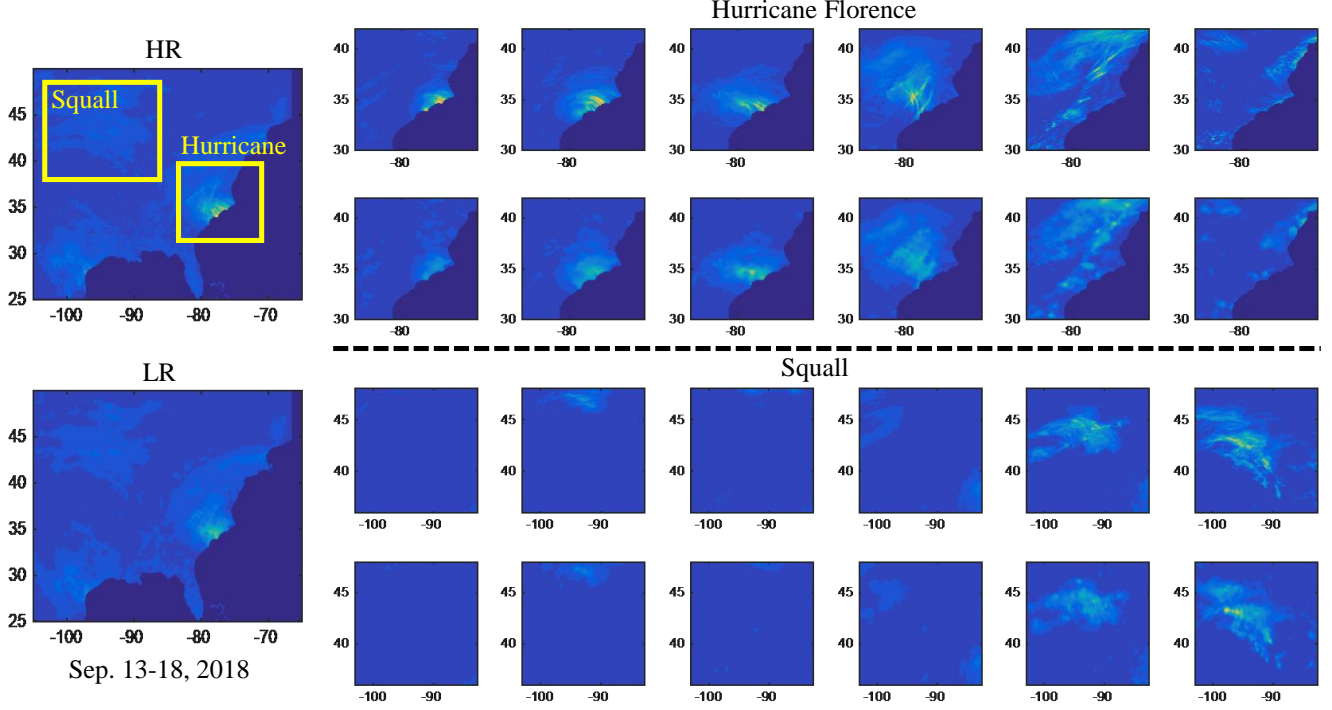


Figure 2. **Dataset Visualization.** Please zoom-in the figure for better observation. Please note that the details of the precipitation map are partially lost due to file compression. Here we plot 2 groups of typical meteorological phenomena (hurricane and squall) in the dataset. To learn more about the dataset, please visit our project website <https://neuralchen.github.io/RainNet/>.

for dynamic, thermodynamic, radiative, and chemical processes working on scales from hundreds of meters to thousands of kilometers and from seconds to weeks [3].

2.1. Meteorological physical model

The Navier–Stokes and mass continuity equations (including the effect of the Earth’s rotation), together with the first law of thermodynamics and the ideal gas law, represent the full set of prognostic equations in the atmosphere, describing the change in space and time of wind, pressure, density and temperature is described (shown in Eq. (1–5)) [3].

Momentum Equations:

$$\begin{aligned} \frac{\partial u}{\partial t} &= -[u, v, w] \cdot \nabla u - \frac{1}{p} \frac{\partial p}{\partial x} + f v, & \text{Zonal} \\ \frac{\partial v}{\partial t} &= -[u, v, w] \cdot \nabla v - \frac{1}{p} \frac{\partial p}{\partial y} - f u, & \text{Meridional} \\ \frac{\partial w}{\partial t} &= -[u, v, w] \cdot \nabla w - \frac{1}{p} \frac{\partial p}{\partial z} - g, & \text{Vertical} \end{aligned} \quad (1)$$

Mass Continuity:

$$\frac{\partial \rho}{\partial t} = -\nabla([u, v, w] \cdot \rho), \quad (2)$$

Thermo-dynamic:

$$\frac{\partial \theta}{\partial t} = -[u, v, w] \cdot \nabla \theta + \dot{Q}, \quad (3)$$

Ideal Gas:

$$p = \rho R T, \quad (4)$$

Moisture equation:

$$\frac{\partial q}{\partial t} = -[u, v, w] \cdot \nabla q + \text{micro}(q). \quad (5)$$

The zonal (u), meridional (v) and vertical (w) wind speed, are driven by air pressure (p). The air pressure is driven by the mass density (ρ , determined by wind and the ingredient of air, *e.g.*, moisture) and the temperature. The moisture and air can contain heat, which forms the variable latent heat (θ). The heat can also come from other heat sources (Q), *e.g.*, physical processes like sun radiation or chemical processes like burning coal. The moisture may also come from snowmelt or other physical processes, which is described in microphysics (*micro*) - a sub-domain of geoscience.

These equations have to be solved numerically using spatial and temporal discretization because of the mathematical intractability of obtaining analytical solutions, and this approximation creates a distinction between so-called resolved and unresolved scales of motion.

2.2. Spatial Down-scaling of Precipitation

The global weather forecast model, treated as a computational problem, relying on high-quality initial data in-

put. The error of weather forecast would increase exponentially over time from this initial error of input dataset. Down-scaling is one of the most important approaches to improve the initial input quality. Precipitation is one of the essential atmospheric variables that are related to daily life. It could easily be observed, by all means, *e.g.*, gauge station, radar, and satellites. Applying down-scaling methods to precipitation and creating high-resolution rainfall is far more meaningful than deriving other variables, while it is the most proper initial task to test deep learning’s power in geo-science. The traditional down-scaling methods can be separated into dynamic and statistical down-scaling.

Dynamic down-scaling treats the down-scaling as an optimization problem constraint on the physical law (described in Eq. (1–5)). The idea of dynamic down-scaling is also a subset of assimilation - the dynamic model meteorologists used to blend different data sources, improve data quality and resolution, and make physical variables constant over time and space. In this way, to downscale a 6 hours of precipitation data, scientists need to run the physical simulation thousands of times, which would take hours on super-computing centers. This computational difficulty also limited the data that scientists could utilize to assimilate and increase the forecast quality. For down-scaling a 7-day precipitation data, people need to simulate the 7-day precipitation for thousand times, which would not be able to finish in days. Thus, this process could not be real-time. As a result, ECMWF(European Centre for Medium-Range Weather Forecasts, one of the most frontier weather forecast centers) can only employ the 6-hour earlier data to increase forecast quality and run four times a day [7].

With such a great effort, the dynamic downscaling methods did not reflect the real-world condition. Instead, these methods find the most likely precipitation over space and time under the pre-defined physical law. Though these physical laws work fluently on coarse data, cases beyond current knowledge also exist when the observation comes to the more in-depth detail of the atmosphere. This fact reminds us that dynamic down-scaling, though works well under current weather forecast system, may not help future forecast system as much as today. A more flexible weather down-scaling framework that could easily blend different sources observations and show the ability to describe more complex physical phenomena on different scales is desperately in need.

Statistical down-scaling is trying to speed up the dynamic down-scaling process. The input of statistical down-scaling is usually dynamic model results or two different observation datasets on different scales. However, due to the quality of statistical downscaling results, people rarely apply statistical down-scaling to weather forecasts. These methods are currently applied in the tasks not requiring high data quality but more qualitative understanding, *e.g.*, cli-

mate projection, which forecasts the weather for hundreds of years on coarse grids and using statistical down-scaling to get detailed knowledge of medium-scale future climate system.

3. RainNet: A Large-scale Spatial Precipitation Downscaling Dataset

3.1. Data Collection and Processing

To build up a standard *realistic (non-simulated)* down-scaling dataset for computer vision, we selected the eastern coast of the United States, which covers a large region (7 million km^2 ; $105^\circ \sim 65^\circ W$, $25^\circ \sim 50^\circ N$) and has a 20-year high-quality precipitation observations. We collected two precipitation data sources from National Stage IV QPE Product (StageIV [21]; high resolution at 0.04° (approximately $4km$)) and North American Land Data Assimilation System (NLDAS [36]; low resolution at 0.125° (approximately $13km$)). StageIV is mosaicked into a national product at National Centers for Environmental Prediction (NCEP), from the regional hourly/6-hourly multi-sensor (radar+gauges) precipitation analyses (MPEs) produced by the 12 River Forecast Centers over the continental United States with some manual quality control done at the River Forecast Centers (RFCs). NLDAS is constructed quality-controlled, spatially-and-temporally consistent datasets from the gauges and remote sensors to support modeling activities. Both products are hourly updated and both available from 2002 to the current age.

In our dataset, we further selected the Eastern coast region for rain season (*July ~ November*, covering hurricane season; hurricanes pour over 10% annual rainfall in less than 10 days). We matched the coordinate system to the lat-lon system for both products and further labeled all the hurricane periods happening in the last 17 years. These heavy rain events are the largest challenge for weather forecasting and downscaling products. As a heavy rain could stimulus a wide-spreading flood, which threatening local lives and arousing public evacuation. If people underestimate the rainfall, a potential flood would be underrated; while over-estimating the rainfall would lead to unnecessary evacuation orders and flood protection, which is also costly.

3.2. Dataset Statistics

At the time of this work, we have collected and processed precipitation data for the rainy season for 17 years from 2002 to 2018. One precipitation map pair per hour, 24 precipitation map pairs per day. In detail, we have collected 85 months or 62424 hours, totaling 62424 pairs of high-resolution and low-resolution precipitation maps. The size of the high-resolution precipitation map is 624×999 , and the size of the low-resolution is 208×333 . Various me-

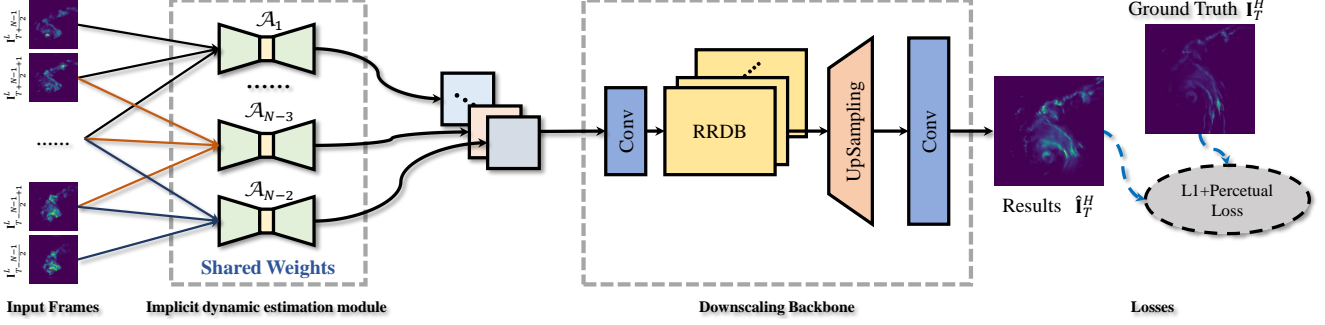


Figure 3. The pipeline of our proposed baseline model for spatial precipitation downscaling.

meteorological phenomena and precipitation conditions (*e.g.*, hurricanes, squall lines, *etc.*) are covered in these data. We select 2 typical meteorological phenomena and visualize them in Fig. 2. Our data is collected from satellites, radars, gauge stations, *etc.*, which covers the inherent working characteristics of different meteorological measurement systems. Compared with traditional methods that generate data with different resolutions through physical model simulation, our dataset is of great help for deep models to learn real meteorological laws.

4. Designing Spatial Downscaling Model

4.1. Dataset Metrics

Due to the difference between downscaling and traditional figure super-resolution, the metrics work well under SR tasks may not be sufficient for precipitation downscaling. Driven by the physical formation of precipitation process, we propose 6 new metrics: mesoscale peak precipitation error (MPPE), heavy rain region error (HRRE), cumulative precipitation mean square error (CPMSE), cluster mean distance (CMD), heavy rain transition speed (HRTS) and average miss moving degree (AMMD). These 6 metrics can be separated as reconstruction metrics: MPPE, HRRE, CPMSE, AMMD and dynamic metrics: HRTS and CMD. The MPPE ($mm/hour$) is calculated as the top 1/1000 quantile difference between the generated/real rainfall dataset which considering both spatial and temporal property of mesoscale meteorological systems, *e.g.*, hurricane, squall. The HRRE (km^2) measures the difference of heavy rain coverage on each time slide between generated and labeled test set, which shows the temporal reconstruction ability of the models. The CPMSE ($mm^2/hour^2$) measures the cumulative rainfall difference on each pixel over the time-axis of the test set, which shows the spatial reconstruction property. The AMMD ($radian$) measures the average angle difference between main rainfall clusters. The CMD (km) compares the location difference of main rainfall system between the generated and labeled test set. The HRTS ($km/hour$) measures the difference between main

rainfall system moving speed between the generated and labeled test set which shows the ability for models to capture the dynamic property. More details about the metrics and their equations are given in supplementary materials. We also included super-resolution metrics such as LPIPS [40] and PSNR to benchmark the model’s ability in reconstructing realistic rainfall. For more detailed information on metrics, please see the suppl.

4.2. Formulation analysis

In order to help design a more appropriate and effective precipitation downscaling model, we have explored the property of the dataset in depth. As mentioned above, our dataset is collected from multiple sensor sources (*e.g.*, satellite, weather radar, *etc.*), which makes the data show a certain extent of *misalignment*. Our efforts here are not able to vanquish the misalignment. This is an intrinsic problem brought by the fusion of multi-sensor meteorological data. Limited by observation methods (*e.g.*, satellites can only collect data when they fly over the observation area), meteorological data is usually *temporal sparse*, *e.g.*, in our dataset, the sampling interval between two precipitation maps is one hour. The temporal sparse leads to serious difficulties in the utilization of precipitation sequences. Additionally, the movement of the precipitation position is directly related to the cloud. It is a fluid movement process which is completely different from the rigid body movement concerned in Super-Resolution. At the same time, the cloud will grow or dissipate in the process of flowing, and even form new clouds, which further complicates the process. In the nutshell, although existed SR is a potential solution for downscaling, there is a big difference between the two. Especially, the three characteristics of downscaling mentioned above: *Temporal Misalignment*, *Temporal Sparse*, *Fluid properties*, which make the dynamic estimation of precipitation more challenging.

4.3. Implicit Dynamic Estimation Model

As a potential solution, *Super-Resolution (SR)* frameworks are generally divided into the Single-Image Super-

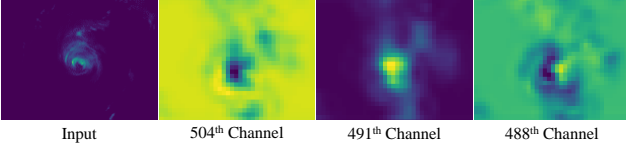


Figure 4. Visualization of the feature map of the precipitation map processed by VGG19. We can see that VGG19 highlights the hurricane eye, which illustrates that the perceptual loss is also effective for the precipitation downscaling task.

Resolution (SISR) and the Video Super-Resolution (VSR). Video Super-Resolution is able to leverage multi-frame information to restore images, which better matches the nature of downscaling. We will demonstrate this judgment in Sec. 5.2. The VSR pipeline usually contains three components: deblurring, inter-frame alignment, and super-resolution. Deblurring and inter-frame alignment are implemented by the motion estimation module. There are four motion estimation frameworks: 1). RNN based [15, 27, 13, 11]; 2). Optical Flow [39]; 3). Deformable Convolution based [29, 37, 32]; 4). Temporal Concatenation [14, 6, 18]. In fact, there is another motion estimation scheme proposed for the first time in the noise reduction task [28], which achieves an excellent video noise reduction performance. Inspired by [28], we design an implicit dynamics estimation model for the spatial precipitation downscaling. It is worth mentioning that our proposed model and the above four frameworks together form a relatively complete candidate set of dynamic estimation solutions.

Proposed Framework. As shown in Fig. 3, our framework consists of two components: *Implicit dynamic estimation module* and *Downscaling Backbone*. These two parts are trained jointly. Suppose there are N adjacent low-resolution precipitation maps $\{\mathbf{I}_{T-\frac{N-1}{2}}^L, \dots, \mathbf{I}_T^L, \dots, \mathbf{I}_{T+\frac{N-1}{2}}^L\}$. The task is to reconstruct the high-resolution precipitation map \mathbf{I}_T^H of \mathbf{I}_T^L . The implicit dynamic estimation module is composed of multiple vanilla networks $\mathcal{A} = \{\mathcal{A}_1, \dots, \mathcal{A}_{N-2}\}$ sharing weights. Each vanilla network receives three adjacent frames as input, outputs and intermediate results. The intermediate result can be considered as a frame with implicit dynamic alignment. We concatenate all the intermediate frames as the input of the next module. The specific structure of the vanilla network can be found in the supplementary materials. The main task of the downscaling backbone is to restore the high-resolution precipitation map \mathbf{I}_T^H based on the aligned intermediate frames. In order to make full use of multi-scale information, we use multiple Residual-in-Residual Dense Blocks [33] in the network. We employ the interpolation+convolution [23] as the up-sampling operator to reduce the checkerboard artifacts. After processing by downscaling backbone we get the final estimated HR map $\hat{\mathbf{I}}_T^H$.

Model objective. The Downscaling task is essentially to restore high-resolution precipitation maps. We learn from the super-resolution task and also apply *L1* and *perceptual loss* as the training loss of our model. The model objective is shown below:

$$\mathcal{L}(\hat{\mathbf{I}}_T^H, \mathbf{I}_T^H) = \|\hat{\mathbf{I}}_T^H - \mathbf{I}_T^H\|_1 + \lambda \|\phi(\hat{\mathbf{I}}_T^H) - \phi(\mathbf{I}_T^H)\|_2, \quad (6)$$

where ϕ denotes the pre-trained VGG19 network [26], we select the *Relu5-4* (without the activator [33]) as the output layer. λ is the coefficient to balance the loss terms.

5. Experiments

5.1. Benchmark

In order to evaluate the effectiveness of the benchmark algorithms, we select the precipitation data from *July to November* 2011 as the benchmark dataset. The benchmark contains 3652 pairs of high-resolution and low-resolution rainfall maps. These data cover various complicated precipitation situations such as hurricanes, squall lines, different levels of rain, and sunny days. It is sufficient to select the rainy season of the year as the test set from the perspective of meteorology, as the climate of one area is normally stable.

5.2. Benchmark Algorithms

The SISR/VSR and the spatial precipitation downscaling are similar to some extent, so we argue that the SR models can be applied to the task as the benchmark models. The input of SISR is a single image, and the model infers a high-resolution image from it. Its main focus is to generate high-quality texture details to achieve pleasing visual effects. In contrast, VSR models input multiple frames of images (*e.g.*, 3 frames, 5 frames, *etc.*). The core idea of VSR models is to increase the resolution by complementing texture information between different frames. It is worth mentioning that VSR models generally are equipped with a *motion estimation module* to alleviate the challenge of object motion to inter-frame information registration. We evaluated 7 state-of-the-art SISR frameworks (*i.e.*, Bicubic [15], SRCNN [8], SRGAN [17], EDSR [19], ESRGAN [33], DBPN [10], RCAN [41]) and 5 VSR frameworks (*i.e.*, SRGAN-V, EDSR-V, ESRGAN-V, RBPN [11], EDVR [32]), of which 3 VSR methods (*i.e.*, SRGAN-V, EDSR-V, ESRGAN-V) are modified from SISR. In particular, we build SRGAN-V, EDSR-V and ESRGAN-V by concatenating multiple frames of precipitation maps as the input of the model. In addition, we also evaluated the traditional statistics method Kriging, which is widely applied in weather forecasting. The mentioned 8 metrics are used to quantitatively evaluate the performance of these SR models

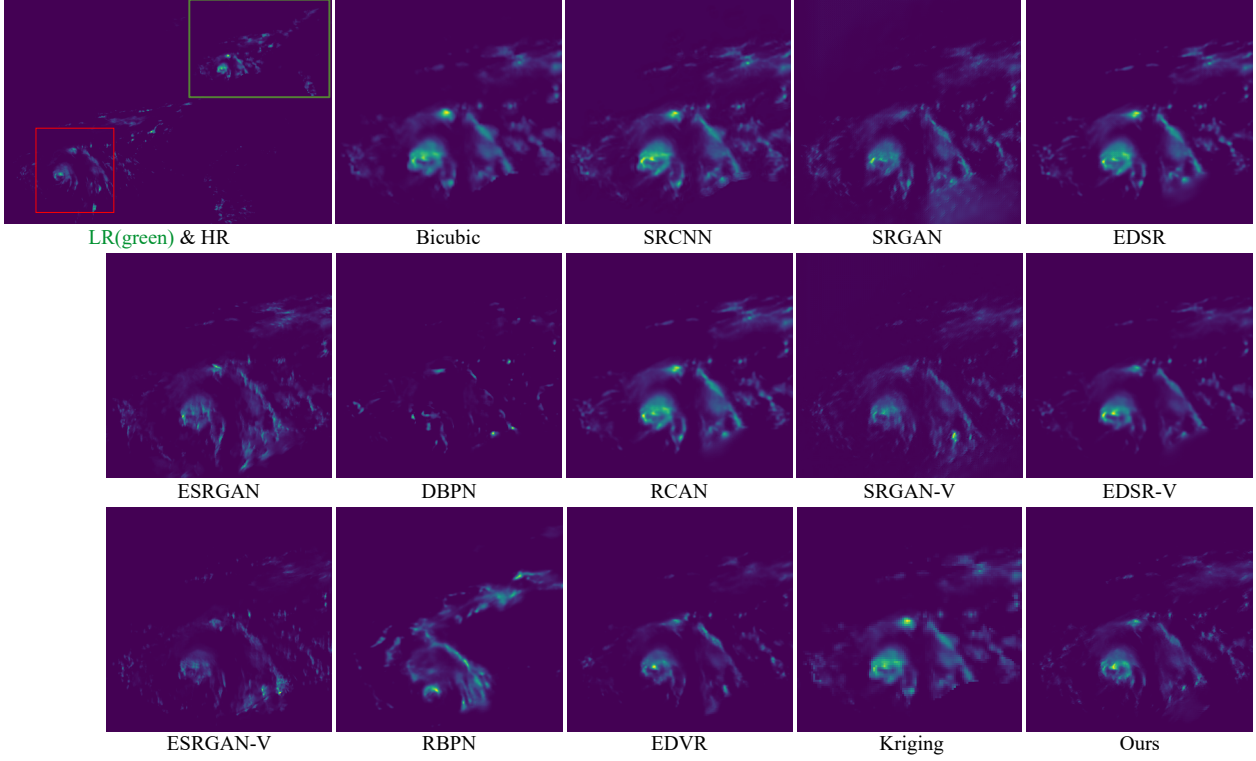


Figure 5. Visual comparison with state-of-the-art Super Resolution approaches. Please zoom-in the figure for better observation. More results can be found in suppl.

Approach	MPPE↓	HRRE↓	AMMD↓	LPIPS↓	PSNR↑	CPMSE↓	HRTS↓	CMD↓
Kriging	0.569	157.716	0.1654	0.0426	49.629	3.590	9.848	11.532
Bicubic	1.688	165.408	0.1759	0.045	50.109	2.518	10.585	11.617
SRCNN	3.301	166.325	0.1871	0.042	48.266	2.150	10.380	11.590
SRGAN	32.34	166.266	0.1834	0.0365	44.361	198.83	8.578	10.439
EDSR	2.526	166.243	0.1601	0.0407	50.587	2.180	9.280	11.533
ESRGAN	15.218	200.694	0.1915	0.0376	47.876	6.292	8.846	10.568
DBPN	3.869	166.340	0.2075	0.0419	48.890	5.3046	9.607	10.994
RCAN	2.557	165.803	0.1521	0.0418	50.612	2.102	8.907	11.575
SRGAN-V	14.21	160.819	0.1636	0.0342	47.858	50.458	7.531	10.409
EDSR-V	2.114	161.048	0.1736	0.0389	50.846	1.9769	7.598	10.470
ESRGAN-V	12.623	329.247	0.187	0.0359	48.361	4.498	7.466	9.767
RBPN	2.181	160.981	0.1674	0.0351	50.826	1.761	7.768	10.371
EDVR	2.113	163.372	0.1684	0.0350	49.826	1.204	8.538	10.627
Ours	1.956	158.569	0.1653	0.0311	50.713	1.461	6.821	10.163

Table 1. Comparison with state-of-the-art Super Resolution approaches. The best performance is marked with **red** (1st best), **blue** (2nd best) and **green** (3rd best).

and our method. Further, we select some disastrous weather as samples for qualitative analysis to test the model’s ability to learn the dynamic properties of the weather system. And we employ the implementation of Pytorch for Bicubic.

5.2.1 Quantitative analysis

We evaluate benchmark frameworks with the benchmark dataset. The downscaling performances are shown in Tab. 1. We divide the indicators mentioned above into two groups. HRTS and CMD together measure the model’s ability to learn the dynamics of precipitation. MPPE, HRRE, AMMD, LPIPS, PSNR and CPMSE indicators illustrate the

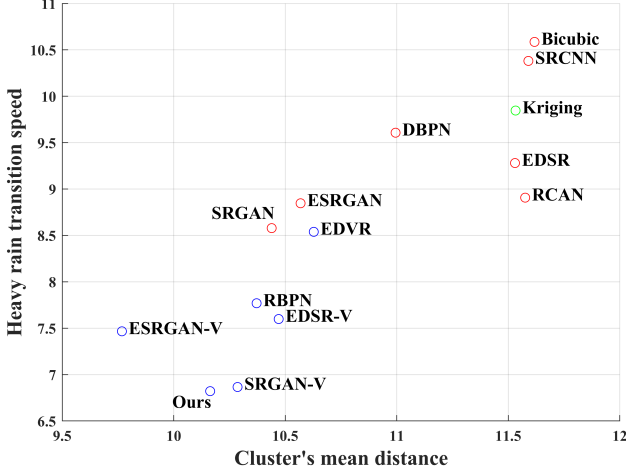


Figure 6. The dynamic property of benchmark algorithms. The frameworks of VSR are gathered in the lower-left corner of the figure, which demonstrates that VSR methods are superior to SISR and traditional methods in dynamic properties.

model’s ability to reconstruct precipitation. From Tab. 1, we can learn that the overall performance of the VSR methods are better than SISR models, which shows that the dynamic properties mentioned above are extremely important for the downscaling model. Furthermore, it can be seen from Fig. 6 that the SISR method is clustered in the upper right corner of the scatter plot, and the VSR method is concentrated in the lower-left corner, which further shows that the dynamic properties of the VSR methods are overall better than the SISR methods. In addition, our method achieves the 1st best performance in LPIPS, HRTS, and achieve the second best performance on HRRE, CPMSE, CMD. The score shows that the implicit dynamic estimation framework used is feasible and effective. It is worth mentioning that the traditional down-scaling method Kriging has achieved the best scores in MPPE and HRRE.

5.2.2 Qualitative analysis

We visualized the hurricane precipitation map of the 166th hour in September 2010 and the high-resolution precipitation map generated by different methods. As shown in Fig. 5, the best perceptual effects are generated by EDVR and Our framework, which is also consistent with the LPIPS score. Zooming-in the result image, the precipitation maps generated by SRGAN and EDSR present obvious checkerboard artifacts. The reason for the checkerboard artifacts should be the relatively simple and sparse texture pattern in precipitation maps. The results generated by Bicubic, RCAN, Kriging and SRCNN are over-smooth. DBPN even cannot reconstruct the eye of the hurricane. Especially, the result generated by Kriging is as fuzzy as the input LR precipitation map. In conclusion, the visual effects generated

by the VSR methods are generally better than the SISR methods and the traditional method. From the perspective of quantitative and qualitative analysis, the dynamics estimation framework is very critical for downscaling.

6. Related Works

Downscaling in Geoscience. Downscaling is a fundamental task in geoscience and meteorology, which researchers have been interested in for a long time [35]. Most statistical downscaling methods regard this problem as point-wise regression [20, 30, 25] or direct maximum likelihood estimation of the high-resolution data from the low-resolution data [2]. Bürger et al. [5] compared bias-correction spatial disaggregation (BCSD), quantile regression networks, and expanded downscaling (XSD) for climate downscaling. Four fundamental statistical methods and three more advanced machine learning methods to downscale daily precipitation in the Northeast United States were compared in [30]. Recently, deep learning methods have been applied to solve the climate downscaling problem. DeepSD [31] tried to employ SRCNN [8] on precipitation downscaling. White *et al* [34] tested the performance of Generative Adversarial Network (GAN) on downscaling weather models. ClimAlign [9] proposed a novel deep learning method for statistical downscaling, treating it as an unsupervised domain alignment problem without using paired low/high resolution training data.

Single Image Super-Resolution(SISR). For deep learning based method, Dong *et al* first proposed an end-to-end model SRCNN [8] using deep convolutional network. SRGAN [17] proposed by Ledig *et al* uses perceptual loss for finer texture. The enhanced version ESRGAN [33] introduces RRDB as basic network unit, using relative discriminator and perceptual loss of features before activation.

Video Super-Resolution(VSR). VSR utilizes the temporal information of image sequences. Wang *et al* proposed a framework EDVR [32], which devises PCD module to handle large motion alignment, and the TSA fusion module with temporal and spatial attention. Xie *et al* proposed the tempoGAN [38] for fluid flow Super-Resolution, synthesizing 4-D physics fields with a temporal discriminator.

7. Conclusion

In this paper, we built the first large-scale *real* precipitation downscaling dataset for the deep learning community. This dataset has 62424 pairs of HR and LR precipitation maps in total. We believe this dataset will further accelerate the research on precipitation downscaling. Furthermore, we analyze the problem in-depth and put forward three key challenges: Temporal Misalignment, Temporal Sparse, Fluid properties. In addition, we propose an implicit dynamic estimation model to alleviate the above challenges.

At the same time, we evaluated the mainstream SISR and VSR models and found that none of these models can solve RainNet’s problems well. Therefore, the downscaling task on this dataset is still very challenging.

References

- [1] Tércio Ambrizzi, Michelle Reboita, Rosmeri Rocha, and Marta Llopart. The state-of-the-art and fundamental aspects of regional climate modeling in south america. *Annals of the New York Academy of Sciences*, 1436, 07 2018.
- [2] Jorge Luis Baño-Medina, Rodrigo García Manzananas, José Manuel Gutiérrez Llorente, et al. Configuration and intercomparison of deep learning neural models for statistical downscaling. 2020.
- [3] Peter Bauer, Alan Thorpe, and Gilbert Brunet. The quiet revolution of numerical weather prediction. *Nature*, 525(7567):47–55, 2015.
- [4] P. Berrisford, D.P. Dee, P. Poli, R. Brugge, Mark Fielding, Manuel Fuentes, P.W. Kållberg, S. Kobayashi, S. Uppala, and Adrian Simmons. The era-interim archive version 2.0. (1):23, 11 2011.
- [5] G Bürger, TQ Murdock, AT Werner, SR Sobie, and AJ Cannon. Downscaling extremes—an intercomparison of multiple statistical methods for present climate. *Journal of Climate*, 25(12):4366–4388, 2012.
- [6] Jose Caballero, Christian Ledig, Andrew P. Aitken, Alejandro Acosta, Johannes Totz, Zehan Wang, and Wenzhe Shi. Real-time video super-resolution with spatio-temporal networks and motion compensation. In *2017 IEEE Conference on Computer Vision and Pattern Recognition, CVPR 2017, Honolulu, HI, USA, July 21-26, 2017*, pages 2848–2857. IEEE Computer Society, 2017.
- [7] PHILIPPE Courtier, J-N Thépaut, and Anthony Hollingsworth. A strategy for operational implementation of 4d-var, using an incremental approach. *Quarterly Journal of the Royal Meteorological Society*, 120(519):1367–1387, 1994.
- [8] Chao Dong, Chen Change Loy, Kaiming He, and Xiaoou Tang. Image super-resolution using deep convolutional networks. *IEEE Trans. Pattern Anal. Mach. Intell.*, 38(2):295–307, 2016.
- [9] Brian Groenke, Luke Madaus, and Claire Monteleoni. Climalign: Unsupervised statistical downscaling of climate variables via normalizing flows. *CoRR*, abs/2008.04679, 2020.
- [10] Muhammad Haris, Gregory Shakhnarovich, and Norimichi Ukita. Deep back-projection networks for super-resolution. In *2018 IEEE Conference on Computer Vision and Pattern Recognition, CVPR 2018, Salt Lake City, UT, USA, June 18-22, 2018*, pages 1664–1673. IEEE Computer Society, 2018.
- [11] Muhammad Haris, Gregory Shakhnarovich, and Norimichi Ukita. Recurrent back-projection network for video super-resolution. In *IEEE Conference on Computer Vision and Pattern Recognition, CVPR 2019, Long Beach, CA, USA, June 16-20, 2019*, pages 3897–3906. Computer Vision Foundation / IEEE, 2019.
- [12] Xiaogang He, Nathaniel W Chaney, Marc Schleiss, and Justin Sheffield. Spatial downscaling of precipitation using adaptable random forests. *Water resources research*, 52(10):8217–8237, 2016.
- [13] Yan Huang, Wei Wang, and Liang Wang. Bidirectional recurrent convolutional networks for multi-frame super-resolution. In *Advances in Neural Information Processing Systems*, pages 235–243, 2015.
- [14] Younghyun Jo, Seoung Wug Oh, Jaeyeon Kang, and Seon Joo Kim. Deep video super-resolution network using dynamic upsampling filters without explicit motion compensation. In *2018 IEEE Conference on Computer Vision and Pattern Recognition, CVPR 2018, Salt Lake City, UT, USA, June 18-22, 2018*, pages 3224–3232. IEEE Computer Society, 2018.
- [15] Robert Keys. Cubic convolution interpolation for digital image processing. *IEEE transactions on acoustics, speech, and signal processing*, 29(6):1153–1160, 1981.
- [16] Mohammad Sajjad Khan, Paulin Coulibaly, and Yonas Dibike. Uncertainty analysis of statistical downscaling methods. *Journal of Hydrology*, 319(1-4):357–382, 2006.
- [17] Christian Ledig, Lucas Theis, Ferenc Huszar, Jose Caballero, Andrew Cunningham, Alejandro Acosta, Andrew P. Aitken, Alykhan Tejani, Johannes Totz, Zehan Wang, and Wenzhe Shi. Photo-realistic single image super-resolution using a generative adversarial network. In *2017 IEEE Conference on Computer Vision and Pattern Recognition, CVPR 2017, Honolulu, HI, USA, July 21-26, 2017*, pages 105–114. IEEE Computer Society, 2017.
- [18] Renjie Liao, Xin Tao, Ruiyu Li, Ziyang Ma, and Jiaya Jia. Video super-resolution via deep draft-ensemble learning. In *2015 IEEE International Conference on Computer Vision, ICCV 2015, Santiago, Chile, December 7-13, 2015*, pages 531–539. IEEE Computer Society, 2015.
- [19] Bee Lim, Sanghyun Son, Heewon Kim, Seungjun Nah, and Kyoung Mu Lee. Enhanced deep residual networks for single image super-resolution. In *2017 IEEE Conference on Computer Vision and Pattern Recognition Workshops, CVPR Workshops 2017, Honolulu, HI, USA, July 21-26, 2017*, pages 1132–1140. IEEE Computer Society, 2017.
- [20] Mohammad Reza Najafi, Hamid Moradkhani, and Susan A Wherry. Statistical downscaling of precipitation using machine learning with optimal predictor selection. *Journal of Hydrologic Engineering*, 16(8):650–664, 2011.
- [21] Brian R. Nelson, Olivier P. Prat, D.-J. Seo, and Emad Habib. Assessment and Implications of NCEP Stage IV Quantitative Precipitation Estimates for Product Intercomparisons. *Weather and Forecasting*, 31(2):371–394, 02 2016.
- [22] NSF. Nsf geosciences directorate funding by institution type. *AGI Report*, 1(1):1–2, 2020.
- [23] Augustus Odena, Vincent Dumoulin, and Chris Olah. Deconvolution and checkerboard artifacts. *Distill*, 1(10):e3, 2016.
- [24] Markus Reichstein, Gustau Camps-Valls, Bjorn Stevens, Martin Jung, Joachim Denzler, Nuno Carvalhais, et al. Deep learning and process understanding for data-driven earth system science. *Nature*, 566(7743):195–204, 2019.

- [25] DA Sachindra, Khandakar Ahmed, Md Mamunur Rashid, S Shahid, and BJC Perera. Statistical downscaling of precipitation using machine learning techniques. *Atmospheric research*, 212:240–258, 2018.
- [26] Karen Simonyan and Andrew Zisserman. Very deep convolutional networks for large-scale image recognition. In Yoshua Bengio and Yann LeCun, editors, *3rd International Conference on Learning Representations, ICLR 2015, San Diego, CA, USA, May 7-9, 2015, Conference Track Proceedings*, 2015.
- [27] Xin Tao, Hongyun Gao, Renjie Liao, Jue Wang, and Jiaya Jia. Detail-revealing deep video super-resolution. In *IEEE International Conference on Computer Vision, ICCV 2017, Venice, Italy, October 22-29, 2017*, pages 4482–4490. IEEE Computer Society, 2017.
- [28] Matias Tassano, Julie Delon, and Thomas Veit. Fastdvdnet: Towards real-time deep video denoising without flow estimation. In *2020 IEEE/CVF Conference on Computer Vision and Pattern Recognition, CVPR 2020, Seattle, WA, USA, June 13-19, 2020*, pages 1351–1360. IEEE, 2020.
- [29] Yapeng Tian, Yulun Zhang, Yun Fu, and Chenliang Xu. TDAN: temporally-deformable alignment network for video super-resolution. In *2020 IEEE/CVF Conference on Computer Vision and Pattern Recognition, CVPR 2020, Seattle, WA, USA, June 13-19, 2020*, pages 3357–3366. IEEE, 2020.
- [30] Thomas Vandal, Evan Kodra, and Auroop R Ganguly. Intercomparison of machine learning methods for statistical downscaling: the case of daily and extreme precipitation. *Theoretical and Applied Climatology*, 137(1-2):557–570, 2019.
- [31] Thomas Vandal, Evan Kodra, Sangram Ganguly, Andrew Michaelis, Ramakrishna Nemani, and Auroop R Ganguly. Deepsd: Generating high resolution climate change projections through single image super-resolution. In *Proceedings of the 23rd acm sigkdd international conference on knowledge discovery and data mining*, pages 1663–1672, 2017.
- [32] Xintao Wang, Kelvin CK Chan, Ke Yu, Chao Dong, and Chen Change Loy. Edvr: Video restoration with enhanced deformable convolutional networks. In *Proceedings of the IEEE Conference on Computer Vision and Pattern Recognition Workshops*, pages 0–0, 2019.
- [33] Xintao Wang, Ke Yu, Shixiang Wu, Jinjin Gu, Yihao Liu, Chao Dong, Yu Qiao, and Chen Change Loy. Esrgan: Enhanced super-resolution generative adversarial networks. In *Proceedings of the European Conference on Computer Vision (ECCV)*, pages 0–0, 2018.
- [34] BL White, A Singh, and A Albert. Downscaling numerical weather models with gans. *AGUFM*, 2019:GC43D–1357, 2019.
- [35] Robert L Wilby, TML Wigley, D Conway, PD Jones, BC Hewitson, J Main, and DS Wilks. Statistical downscaling of general circulation model output: A comparison of methods. *Water resources research*, 34(11):2995–3008, 1998.
- [36] Youlong Xia, Kenneth Mitchell, Michael Ek, Justin Sheffield, Brian Cosgrove, Eric Wood, Lifeng Luo, Charles Alonge, Helin Wei, Jesse Meng, Ben Livneh, Dennis Lettenmaier, Victor Koren, Qingyun Duan, Kingtse Mo, Yun Fan, and David Mocko. Continental-scale water and energy flux analysis and validation for the north american land data assimilation system project phase 2 (nldas-2): 1. intercomparison and application of model products. *Journal of Geophysical Research: Atmospheres*, 117(D3), 2012.
- [37] Xiaoyu Xiang, Yapeng Tian, Yulun Zhang, Yun Fu, Jan P. Allebach, and Chenliang Xu. Zooming slow-mo: Fast and accurate one-stage space-time video super-resolution. In *2020 IEEE/CVF Conference on Computer Vision and Pattern Recognition, CVPR 2020, Seattle, WA, USA, June 13-19, 2020*, pages 3367–3376. IEEE, 2020.
- [38] You Xie, Erik Franz, Mengyu Chu, and Nils Thuerey. tempogan: A temporally coherent, volumetric gan for super-resolution fluid flow. *ACM Transactions on Graphics (TOG)*, 37(4):1–15, 2018.
- [39] Tianfan Xue, Baian Chen, Jiajun Wu, Donglai Wei, and William T. Freeman. Video enhancement with task-oriented flow. *Int. J. Comput. Vis.*, 127(8):1106–1125, 2019.
- [40] Richard Zhang, Phillip Isola, Alexei A Efros, Eli Shechtman, and Oliver Wang. The unreasonable effectiveness of deep features as a perceptual metric. In *Proceedings of the IEEE conference on computer vision and pattern recognition*, pages 586–595, 2018.
- [41] Yulun Zhang, Kunpeng Li, Kai Li, Lichen Wang, Bineng Zhong, and Yun Fu. Image super-resolution using very deep residual channel attention networks. In Vittorio Ferrari, Martial Hebert, Cristian Sminchisescu, and Yair Weiss, editors, *Computer Vision - ECCV 2018 - 15th European Conference, Munich, Germany, September 8-14, 2018, Proceedings, Part VII*, volume 11211 of *Lecture Notes in Computer Science*, pages 294–310. Springer, 2018.

Appendix: Supplementary Material

In this supplementary material, we illustrate the details of proposed metrics and provide more samples of our dataset. Furthermore, we discuss the configuration of training and report more experimental results. We will publish the dataset and code on <https://neuralchen.github.io/RainNet/>.

A. Metrics

Due to the difference between downscaling and traditional figure super-resolution, the metrics work well under SR tasks may not be sufficient for precipitation downscaling. Driven by the physical formation of precipitation process, we propose 6 new metrics: mesoscale peak precipitation error (MPPE), heavy rain region error (HRRE), cumulative precipitation mean square error (CPMSE), cluster mean distance (CMD), heavy rain transition speed (HRTS) and average miss moving degree (AMMD). These 6 metrics can be separated as reconstruction metrics: MPPE, HRRE, CPMSE, AMMD and dynamic metrics: HRTS and CMD. The MPPE ($mm/hour$) is calculated as the top 1/1000 quantile difference between the generated/real rainfall dataset which considering both spatial and temporal property of mesoscale meteorological systems, *e.g.*, hurricane, squall. The HRRE (km^2) measures the difference of heavy rain coverage on each time slide between generated and labeled test set, which shows the temporal reconstruction ability of the models. The CPMSE ($mm^2/hour^2$) measures the cumulative rainfall difference on each pixel over the time-axis of the test set, which shows the spatial reconstruction property. The AMMD (*radian*) measures the average angle difference between main rainfall clusters. The CMD (km) compares the location difference of main rainfall system between the generated and labeled test set. The HRTS ($km/hour$) measures the difference between main rainfall system moving speed between the generated and labeled test set which shows the ability for models to capture the dynamic property. More details about the metrics and their equations are given in supplementary materials.

These metrics follows different formulations under the test set time length T and test set area size A :

Mesoscale peak precipitation error (MPPE) This metric measures the ability for the downscaling models to capture the mesoscale peak precipitation. The mesoscale large weather/meteorological events are happening on a scale of $200km \times 200km$, such as hurricane or squall. The ability of capturing this metrics would help improve the flood prediction, as the precipitation events at this scale could stimulus large flooding. By measuring 1/1000 quantile of precipitation ($5000 km^2$) over temporal and spatial, we could capture the precipitation at the mesoscale weather events.

Heavy rain region error (HRRE) This metric measures the difference between the reconstructed dataset and the real high-resolution observations of the heavy rain region. The heavy rain is defined by $56mm/day$, which is a conventional benchmark for heavy rain in weather prediction (America: $50.8 - 76.2mm/day$; Japan, India and China: $50 - 75mm/day$; European: $40 - 60mm/day$). This metrics is formed by:

$$HRRE = (\frac{1}{T} \sum_t (A_{HR}(P > 56, t) - A_{GT}(P > 56, t))^2)^{0.5},$$

where HR means the high-resolution data and GT is the generated data.

Cumulative precipitation mean square error (CPMSE)

This metric represents the ability for model to capture the spatial difference of precipitation over a long time, which is usually considered in climatology. Through long time observation, we use this metrics to lay out the impact of miss alignment issue and focus on the climatology and spatial rainfall estimation. This metric is formed by:

$$CPMSE = (\frac{1}{T \cdot A} \sum_{ij} (\sum_t P_{HR}(i, j, t) - \sum_t P_{GT}(i, j, t))^2)^{0.5}.$$

Cluster mean distance (CMD) This metric measures the distance between the main rainfall clusters between the generated dataset and the high-resolution. This metric block the rainfall quantity estimation error and focusing on spatial difference on each time slide. For each frame, we first calculate out the area size of the heavy rain in HR dataset. We mark the contour of heavy rain in HR dataset as $f_{HR}(x, y, t)$. The area of this contour is marked as A_{Rain} . Then we find the contour of generated rainfall dataset with the same area size as in $f_{HR}(x, y, t)$ and mark the contour as $f_{GT}(x, y, t)$. We calculate out the heavy rain contour difference between HR and GT dataset under 2-norm. The metrics could be calculated as:

$$CMD = (\sum_t \frac{1}{T \cdot A_{Rain}} < \iint [x, y] f_{HR}(x, y, t) - [x, y] f_{GT}(x, y, t) dx dy >)^{0.5}.$$

In which \oint is the area integration; $<>$ means the self inner product.

To further calculate this value, we need to discrete this value as:

$$CMD = (\sum_t \frac{1}{T \cdot A_{Rain}} < \sum_i \sum_j [i, j] f_{HR}^D(i, j, t) - [i, j] f_{GT}^D(i, j, t) >)^{0.5},$$

where f_*^D becomes 1 when the lattices are on the boundary of the contours; otherwise it would be 0.

Average miss moving degree (AMMD) These metrics measures the ability for model to capture the temporal direction of heavy rain. For each frame, we first calculate out the area size of the heavy rain in HR dataset. We mark the contour of heavy rain in HR dataset as $f_{HR}(x, y, t)$. Then for the last frame in HR dataset, we find the contour of generated rainfall dataset with the same size. We calculate out the heavy rain contour's outer normal difference between this and last frame, which has the physical meaning - moving angle of rain clusters. Then we compare the difference of HR and GT under 2-norm. We also do this for the generated dataset. The metrics could be calculated as:

$$AMMD = (\sum_t \frac{1}{T \cdot A_{Rain}} < \nabla_t \oint f_{HR}(x, y, t) dr_{HR} - \oint f_{GT}(x, y, t) \cdot dr_{GT} >)^{0.5}.$$

To further calculate this value, we need to discrete this value as:

$$AMMD = (\sum_t \frac{1}{T \cdot A_{Rain}} < \sum_i \sum_j (f_{HR}^O(i, j, t) - f_{HR}^O(i, j, t-1)) - \sum_i \sum_j (f_{GT}^O(i, j, t) - f_{GT}^O(i, j, t-1)) >)^{0.5},$$

where f_*^O is the outer normal direction (unitized) of the contours.

Heavy rain transition speed (HRTS) These metrics measures the ability for model to capture the dynamics (transition speed) of heavy rain. For each frame, we first calculate out the area size of the heavy rain in HR dataset. We mark the contour of heavy rain in HR dataset as $f_{HR}(x, y, t)$. Then for the last frame in HR dataset, we find the contour of generated rainfall dataset with the same size. We also do this for the generated dataset. We calculate out the heavy rain contour difference between this and last frame. Then we compare the difference of HR and GT under 2-norm. This metrics actually shows the order-1 property of dynamics which is shown in main text Eq.1 - the wind blowing effect. The metrics could be calculated as:

$$HRTS = (\sum_t \frac{1}{T \cdot A_{Rain}} < \nabla_t \iint [x, y] f_{HR}(x, y, t) - [x, y] f_{GT}(x, y, t) dx dy >)^{0.5}.$$

To further calculate this value, we need to discrete this value as:

$$HRTS = (\sum_t \frac{1}{T \cdot A_{Rain}} < \sum_i \sum_j [i, j] (f_{HR}(i, j, t) - f_{HR}(i, j, t-1)) - [i, j] (f_{GT}(i, j, t) - f_{GT}(i, j, t-1)) >)^{0.5}.$$

B. Dataset Details

We show more precipitation maps in proposed dataset. In order to display the dynamic characteristics of the precipitation map more conveniently, we extract the precipitation maps of 4 periods and make them into GIFs. These GIFs are organized in the attachment of the supplementary materials.

C. Extra Results of RainNet

C.1. Detailed Network Structure

The structure of vanilla network in our proposed framework is given in Fig. 7. We employ 6 Residual-in-Residual Dense Blocks(RRDB) [33] in our vanilla network.

C.2. Training Details

We select 13 Algorithms as Benchmark: Bicubic [15], SRCNN [8], SRGAN [17], EDSR [19], ESRGAN [33], DBPN [10], RCAN [41], SRGAN-V, EDSR-V, ESRGAN-V, RBPN [11], EDVR [32] and Kriging. These implementations are derived or adapted from publicly available code provided by the authors. Since all these methods process three-channel pictures by default, we modify the number of input channels of these models (The precipitation map in our proposed dataset are all single-channel). According to our task, we also adjust the hype parameters of these models for better performance.

C.3. Extra Results

We randomly pick 6 sets of results and show them in Fig. 8~13. In addition, we extract the downscaling results (our proposed method) of 5 periods and make them into GIFs. These GIFs are organized in the attachment of the supplementary materials.

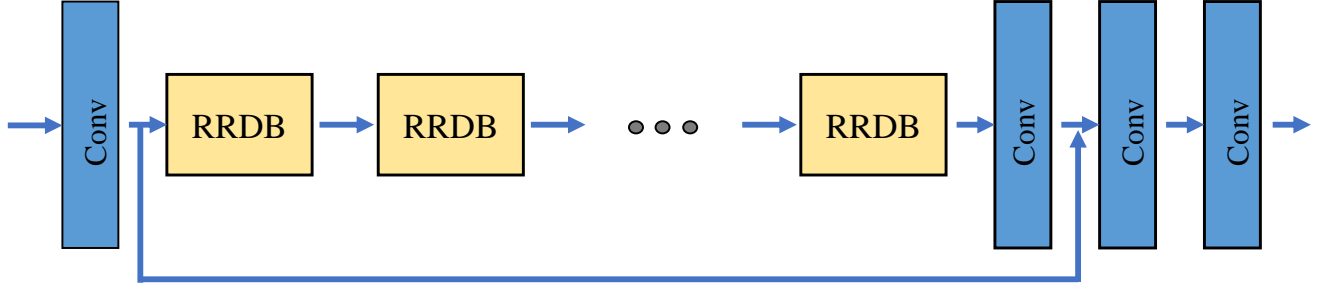


Figure 7. The details structure of vanilla network in our proposed model.

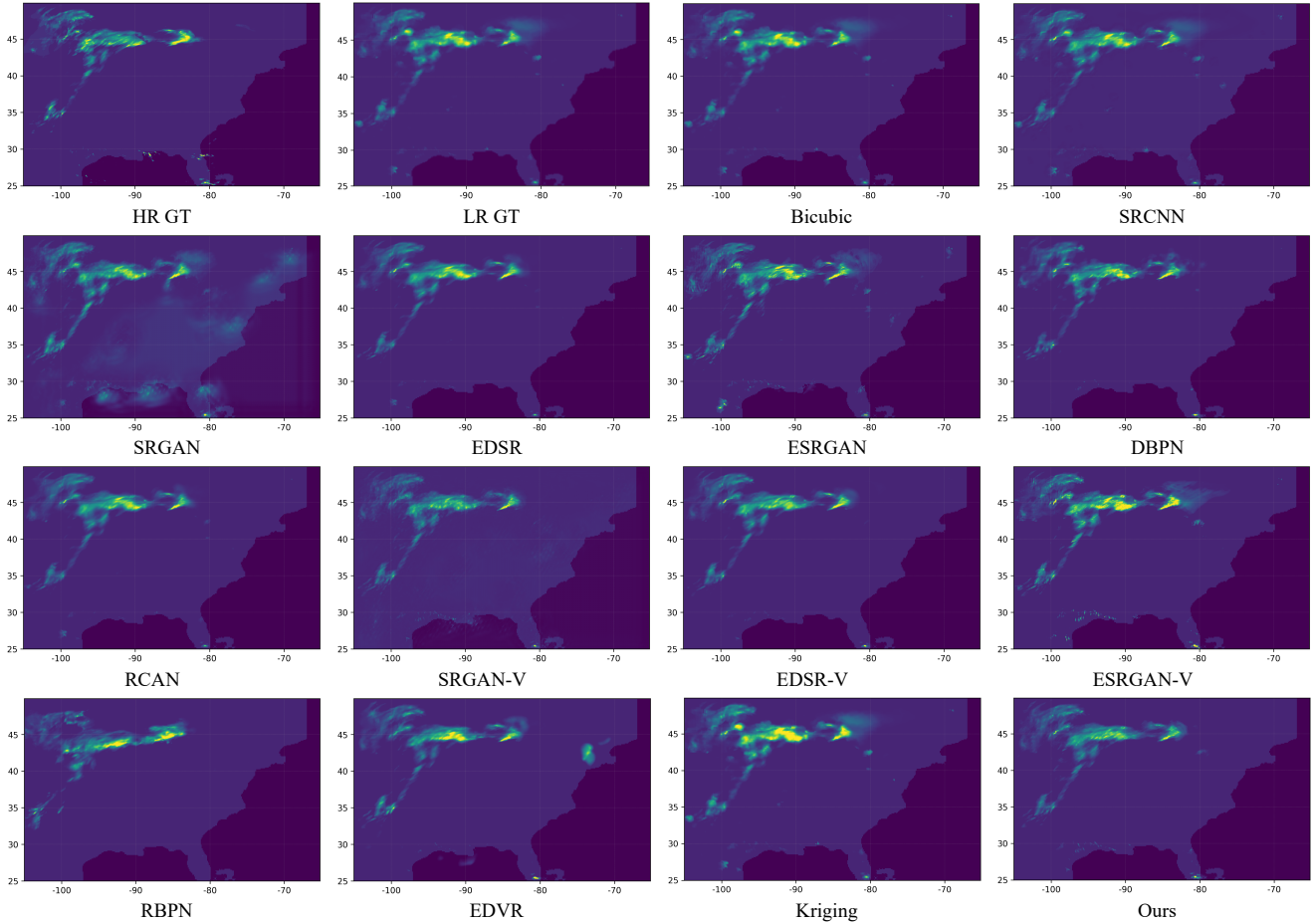


Figure 8. Visual comparison with state-of-the-art Super Resolution approaches(the specific time: the 546-th hour in September 2010). Please zoom-in the figure for better observation. Randomly picked results. Please note that the details of the precipitation map are partially lost due to file compression.

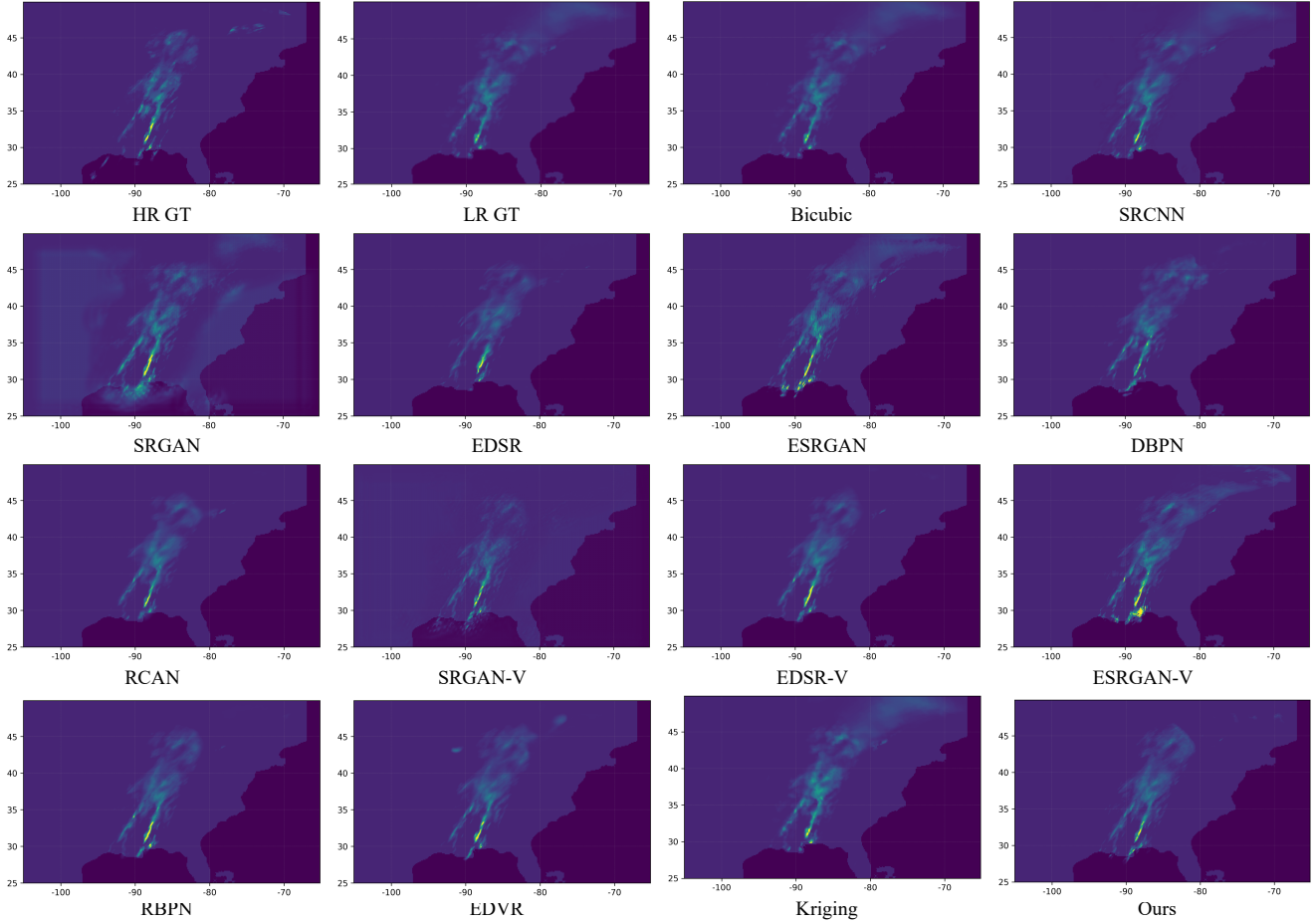


Figure 9. Visual comparison with state-of-the-art Super Resolution approaches(the specific time: the 635-th hour in November 2011). Please zoom-in the figure for better observation. Randomly picked results. Please note that the details of the precipitation map are partially lost due to file compression.

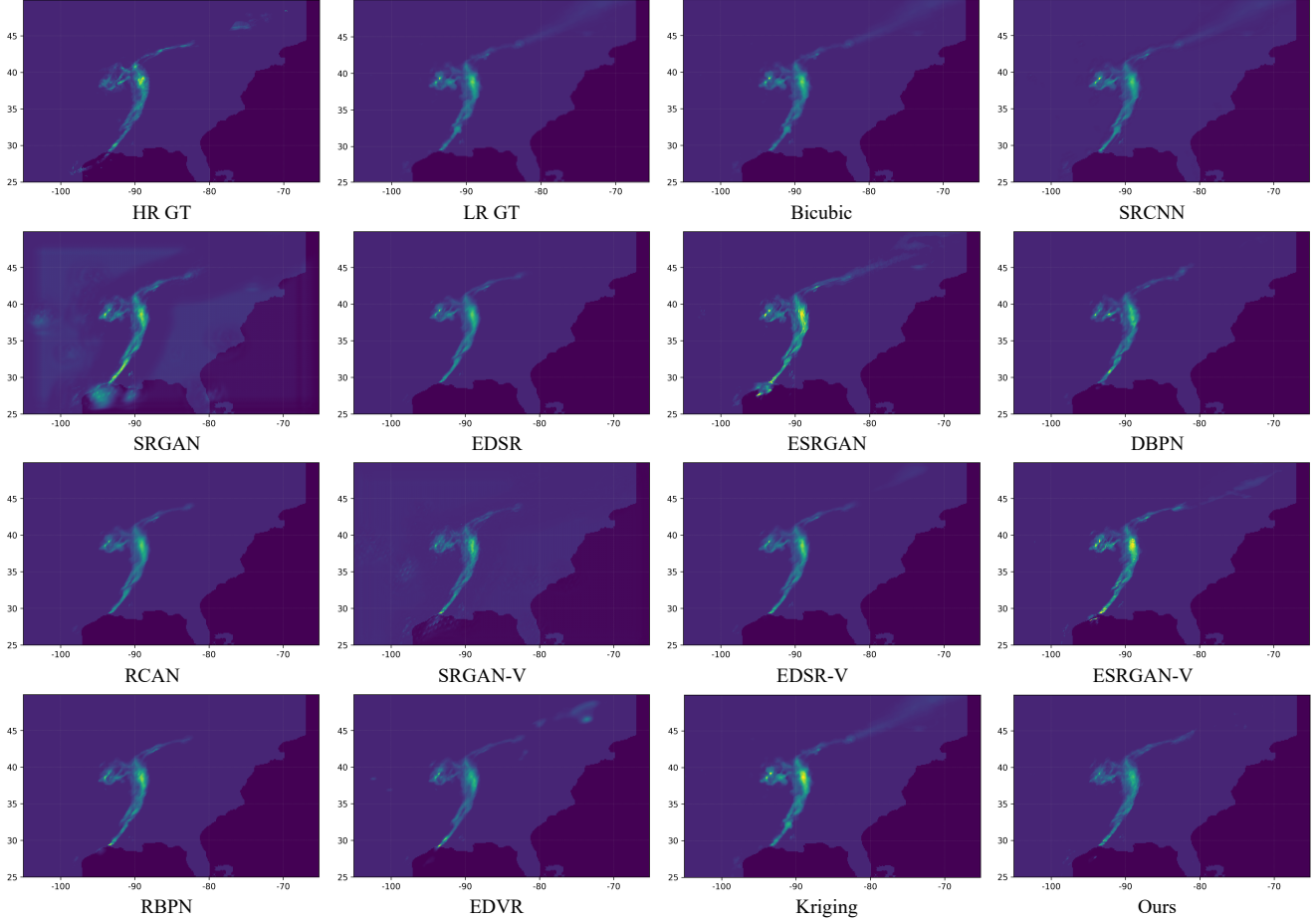


Figure 10. Visual comparison with state-of-the-art Super Resolution approaches(the specific time: the 59-th hour in November 2011). Please zoom-in the figure for better observation. Randomly picked results. Please note that the details of the precipitation map are partially lost due to file compression.

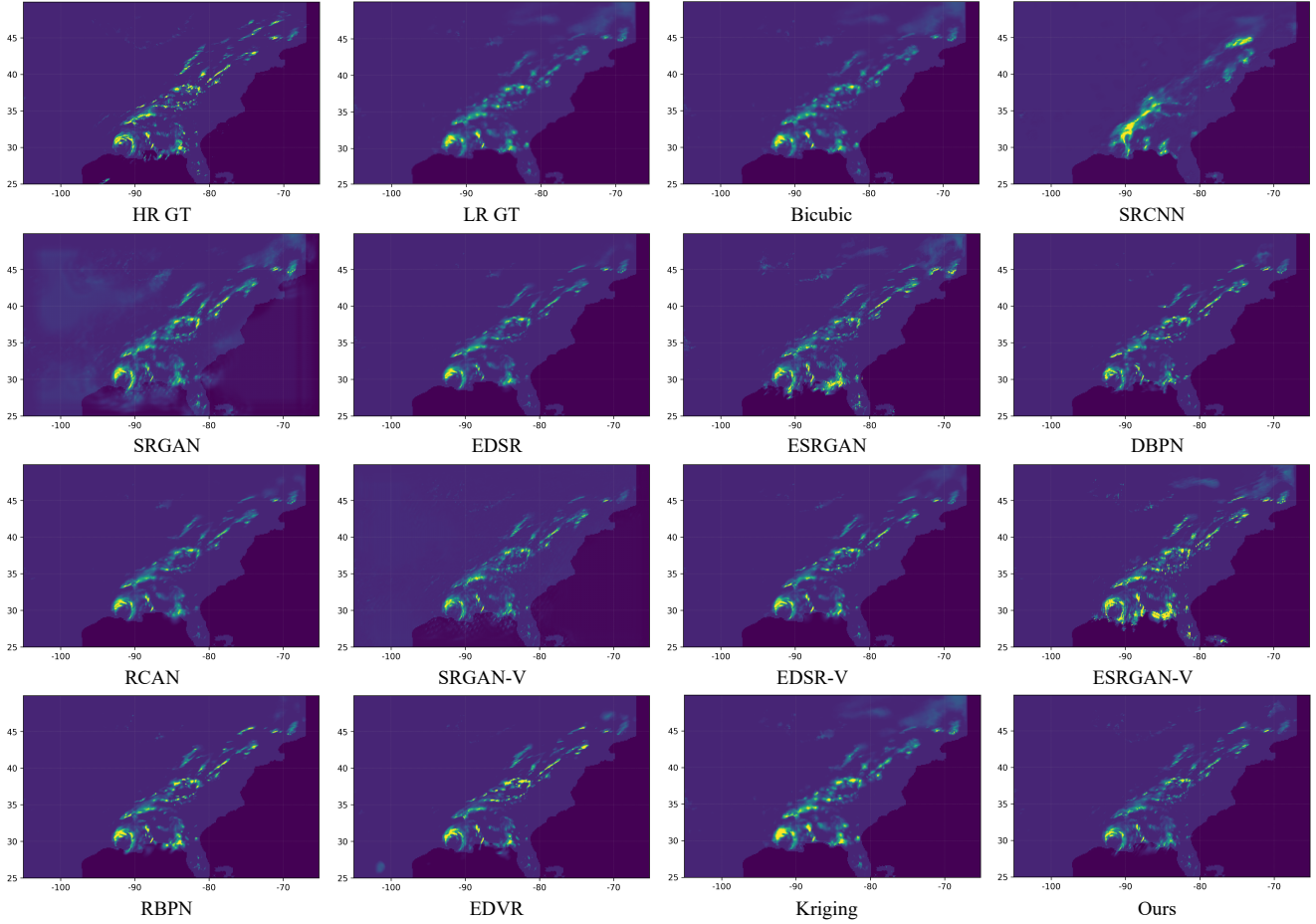


Figure 11. Visual comparison with state-of-the-art Super Resolution approaches(the specific time: the 95-th hour in September 2011). Please zoom-in the figure for better observation. Randomly picked results. Please note that the details of the precipitation map are partially lost due to file compression.

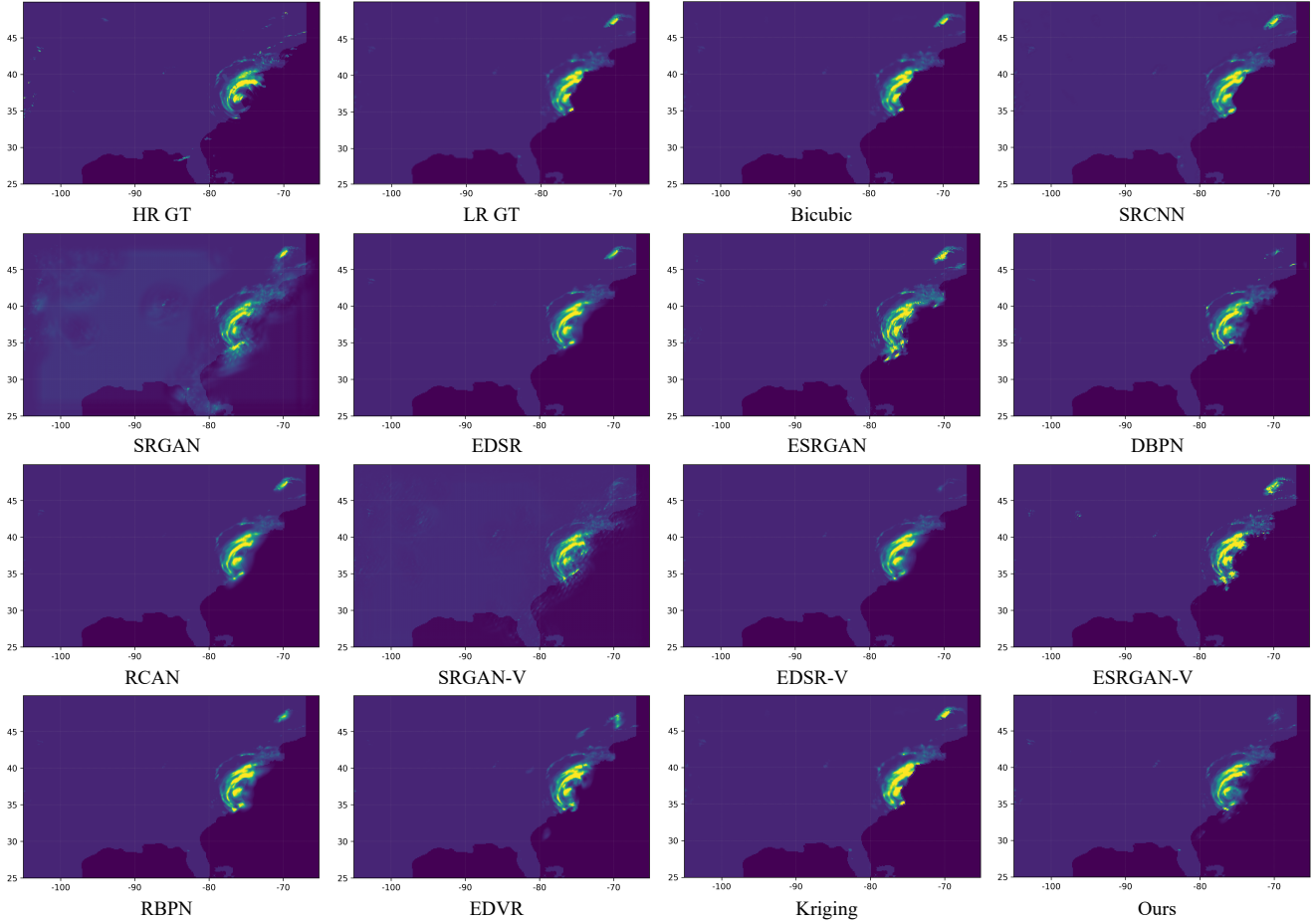


Figure 12. Visual comparison with state-of-the-art Super Resolution approaches(the specific time: the 649-th hour in August 2011). Please zoom-in the figure for better observation. Randomly picked results. Please note that the details of the precipitation map are partially lost due to file compression.

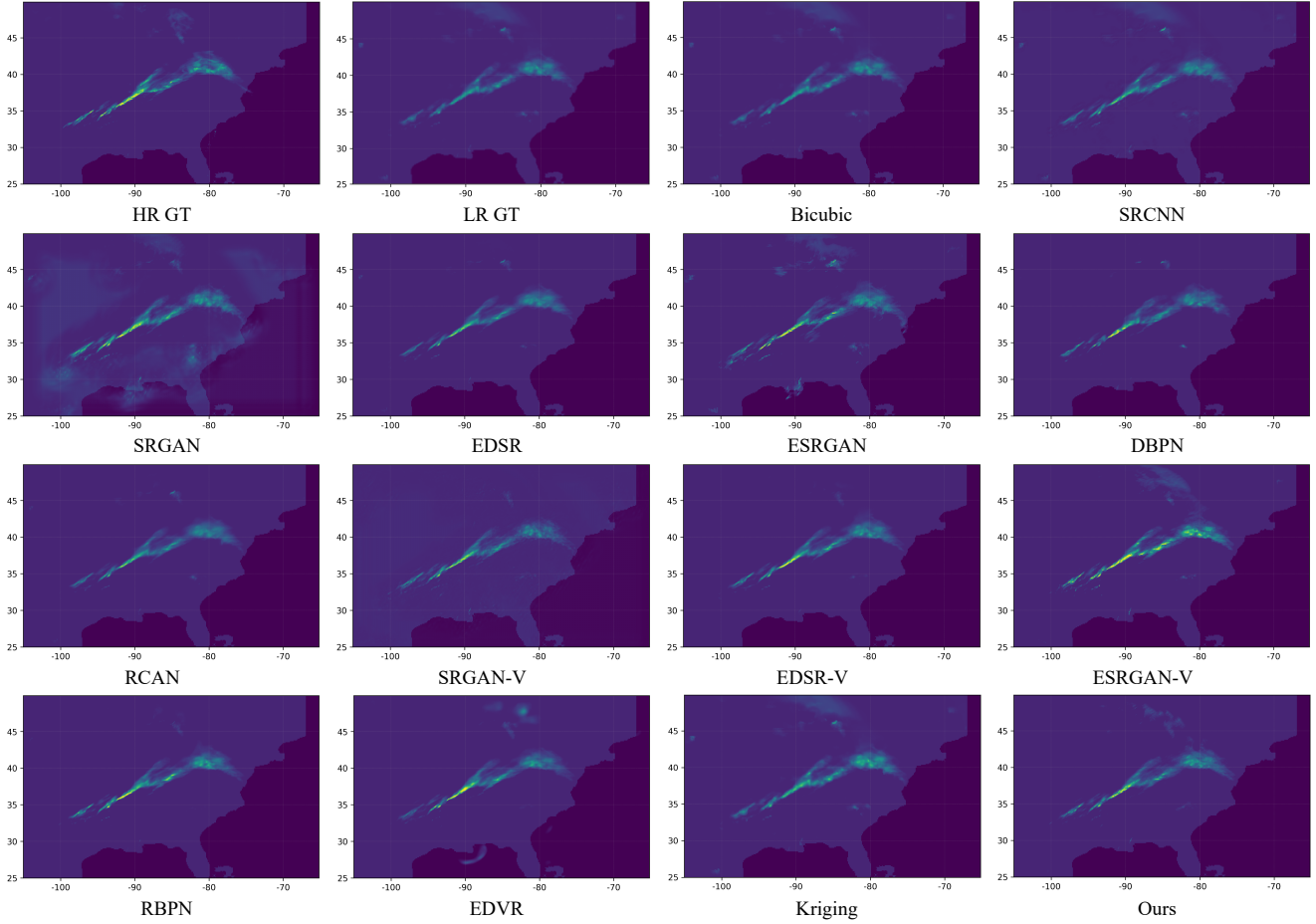


Figure 13. Visual comparison with state-of-the-art Super Resolution approaches(the specific time: the 590-th hour in November 2010). Please zoom-in the figure for better observation. Randomly picked results. Please note that the details of the precipitation map are partially lost due to file compression.